Laboratory Investigation (2020) 100:696–711
https://doi.org/10.1038/s41374-019-0360-4

ARTICLE

Role of cyclin-dependent kinase 2 in the progression of mouse juvenile cystic kidney disease

Jennifer Qin Jing Zhang[1,2] · Jane Burgess[1,2] · Daria Stepanova[1,2] · Sayanthooran Saravanabavan[1,2] · Annette T. Y. Wong[1,2] · Philipp Kaldis[3,4] · Gopala K. Rangan[1,2]

Received: 28 September 2018 / Revised: 29 August 2019 / Accepted: 4 September 2019 / Published online: 8 January 2020

Abstract

A hallmark of polycystic kidney diseases (PKDs) is aberrant proliferation, which leads to the formation and growth of renal cysts. Proliferation is mediated by cyclin-dependent kinases (Cdks), and the administration of roscovitine (a pan-Cdk inhibitor) attenuates renal cystic disease in juvenile cystic kidney (*jck*) mice. *Cdk2* is a key regulator of cell proliferation, but its specific role in PKD remains unknown. The aim of this study was to test the hypothesis that *Cdk2* deficiency reduces renal cyst growth in PKD. Three studies were undertaken: (i) a time course (days 28, 56, and 84) of cyclin and Cdk activity was examined in *jck* mice and compared with wild-type mice; (ii) the progression was compared in *jck* mice with or without *Cdk2* ablation from birth; and (iii) the effect of sirolimus (an antiproliferative agent) on *Cdk2* activity in *jck* mice was investigated. Renal disease in *jck* mice was characterized by diffuse tubular cyst growth, interstitial inflammation and fibrosis, and renal impairment, peaking on day 84. Renal cell proliferation peaked during earlier stages of disease (days 28–56), whereas the expression of *Cdk2*-cyclin partners (A and E) and *Cdk1* and *2* activity, was maximal in the later stages of disease (days 56–84). *Cdk2* ablation did not attenuate renal disease progression and was associated with persistent *Cdk1* activity. In contrast, the postnatal treatment of *jck* mice with sirolimus reduced both *Cdk2* and *Cdk1* activity and reduced renal cyst growth. In conclusion, (i) the kinetics of *Cdk2* and *Cdk2*-cyclin partners did not correlate with proliferation in *jck* mice; and (ii) the absence of *Cdk2* did not alter renal cyst growth, most likely due to compensation by *Cdk1*. Taken together, these data suggest that *Cdk2* is dispensable for the proliferation of cystic epithelial cells and progression of PKD.

Introduction

Polycystic kidney diseases (PKDs) are a common cause of end-stage kidney disease (ESKD) and account for ~10% of patients requiring dialysis or transplantation [1, 2]. They are characterized by the asynchronous or synchronized formation of numerous cysts (or cystic tubular dilatation) in the kidney, accompanied by fibrosis, inflammation, and the loss of normal kidney tissue [2]. PKDs are mostly hereditary, caused by single gene germ-line mutations, but can also arise randomly due to developmental defects or be acquired in adulthood [1]. The main types of PKD include autosomal dominant and recessive PKD, nephronophthisis, and medullary cystic disease, all of which exhibit variations in disease phenotype [1]. The most common form, autosomal dominant PKD (ADPKD), has a population prevalence of 1:1000 and is caused by mutations in either *PKD1* or *PKD2* [2, 3]. These genes encode the proteins, polycystin-1 and 2, which localize to the primary cilia, classifying ADPKD as a

Supplementary information The online version of this article (https://doi.org/10.1038/s41374-019-0360-4) contains supplementary material, which is available to authorized users.

✉ Jennifer Qin Jing Zhang
jennifer.zhang@sydney.edu.au

[1] Centre for Transplant and Renal Research, Westmead Institute for Medical Research, The University of Sydney, 176 Hawkesbury Road, PO Box 412, Westmead, NSW 2145, Australia

[2] Department of Renal Medicine, Westmead Hospital, Westmead, NSW 2145, Australia

[3] Institute of Molecular and Cell Biology (IMCB), A*STAR (Agency for Science Technology and Research), Singapore 138673, Republic of Singapore

[4] Department of Biochemistry, National University of Singapore (NUS), Singapore 117597, Republic of Singapore

renal "ciliopathy" [3, 4]. Long-term complications of ADPKD include bilateral kidney enlargement, the progressive loss of renal function and extra-renal manifestations (such as hypertension, polycystic liver disease, and intracranial aneurysms) [1, 2]. Autosomal recessive PKD (ARPKD) is much less common (1:20,000 population prevalence), and typically results in fetal or neonatal death due to enormous kidney enlargement and impaired pulmonary development [1]. At present, current treatments are limited, and more effective therapies are required to prevent ESKD.

Over the last 20 years, there has been an increasing interest in targeting the cell-cycle regulation as a potential approach to reduce the abnormal proliferation of cystic epithelial cells (CECs) in PKD. A hallmark of PKDs is an increased capacity for proliferation, dedifferentiation, and the survival of epithelial cells lining the renal cysts, which allow for their persistent expansion [1]. At a molecular level, cell proliferation in mammalian cells is governed by progression through the cell cycle, allowing cell division to occur. As shown in Fig. 1, the cell cycle consists of four phases (G_1, S, G_2, and M), and progression through each phases is governed by regulatory proteins, mainly cyclin-dependent kinases (Cdks) and their partner subunits, cyclins [5]. Five different Cdks (*Cdk1–4, 6*) have a direct role in regulating the cell cycle [5]. The *Cdk2*-cyclin E complex is involved in initiating DNA replication and phosphorylating retinoblastoma (Rb) proteins, to allow progression from G_1 to S phase (Fig. 1) [6, 7]. *Cdk2* also partners with cyclin A to potentiate progression through S phase [6, 7], suggesting that *Cdk2* has a major role in the cell cycle, cell division, and proliferation of CECs (Fig. 1). However, *Cdk2* knockout mice are viable indicating that *Cdk2* is dispensable for the proliferation and survival of most cell types during development [8, 9]. *Cdk5* does not have a direct role in regulating proliferation via cell cycle [6], and a recent study by Husson et al. [10] indicates that it is required for maintaining primary cilia and epithelial cell differentiation in PKD via its downstream target, collapsin response mediator protein 2 (CRMP2) (Fig. 1).

Previous studies have suggested that *Cdk2* may have a specific role in mediating CEC proliferation in PKD. In vitro, polycystin-1 inhibited *Cdk2* activity, but had no effect on *Cdk4* or *Cdk6* or any of their associated cyclins [11]. Furthermore, *Cdk2* levels were upregulated 2.2-fold in primary tubular epithelial cells isolated from *PKD2* transgenic rats [12]. Bukanov et al. [13] also demonstrated that the pan-Cdk inhibitor, *R*-roscovitine, inhibited cystogenesis in two animal models of PKD (*jck* and *cpk* mice). Lastly, the administration of (*R*)-roscovitine and S-CR8 (a more potent and selective Cdk inhibitor) attenuated cystic disease in a genetic orthologue of ADPKD (*PKD1* conditional knockout mice) [14]. These data suggest that *Cdk2* has a specific pathogenetic role in the progression of PKD, but direct evidence is lacking.

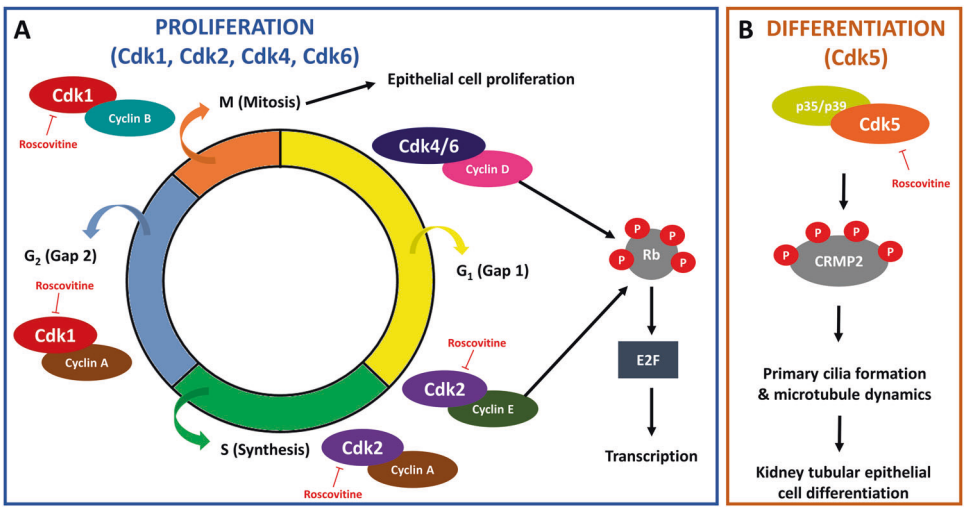

Fig. 1 The roles of cyclin-dependent kinase (Cdk) and cyclin complexes in polycystic kidney disease (PKD). a Epithelial cell proliferation, *Cdk4/6*-cyclin D is involved in the early stages of G_1 and conducts the initial phosphorylation of retinoblastoma protein (pRb) [6]. *Cdk2*-cyclin E complexes complete the phosphorylation of pRb and potentiate progression from G_1 to S by facilitating the localization of proteins onto origins of replication. The phosphorylation of pRb activates the transcription factor, E2F, which acts on numerous targets to increase the expression of cyclins and Cdks, as well as proteins for DNA repair and replication, all required for entry into S phase [7]. *Cdk2*-cyclin A is required for progression through S phase. *Cdk1*-cyclin A acts on proteins involved in DNA replication and cell-cycle control to allow transition from S to G_2 phase, and *Cdk1*-cyclin B is required for mitosis (i.e., transition from G_2 to M) to occur [6]. In contrast, **b** Cdk5 regulates epithelial cell differentiation. Cdk5 is activated by non-cyclin proteins, p35 and p39, and does not directly regulate proliferation via cell cycle [6]. However, recent evidence suggests that in PKD, *Cdk5* mediates epithelial cell differentiation via phosphorylation of its downstream effector, collapsin response mediator protein 2 (CRMP2) [10]. Treatment with roscovitine inhibits *Cdk1*, *Cdk2*, and *Cdk5* activity [39]. *Cdk* cyclin-dependent kinase.

The juvenile cystic kidney (*jck)* disease mouse model is mediated by a point mutation in *Nek8* [15]. *Nek8* is a mitotic kinase, linked to both ADPKD and ARPKD, as it regulates intracellular levels of polycystins [16], and is mutated in human nephronophthisis [17]. In the present study, we examined the hypothesis that the progression of cystic renal disease in *jck* mice is reduced in the absence of *Cdk2*. The specific aims of the current study were to: (i) determine the kinetics of cell-cycle-associated Cdks and cyclins in *jck* mice; (ii) generate compound mice that were homozygous for both the *jck* mutation and *Cdk2* gene deletion; (iii) assess the effect of *Cdk2* deficiency on the progression of cystic renal disease in these animals; and (iv) examine the effect of sirolimus, an anti-proliferative agent, on the cell cycle-associated Cdks and cyclins.

Materials and methods

Animal models

jck C57BL/6J mice

jck mice [18] were obtained from The Jackson Laboratory (Stock #002561; Bar Harbor ME, USA) and used to establish a breeding colony at the Westmead Hospital animal facility (Sydney NSW, Australia). Animals homozygous for the mutated *Nek8* gene develop polycystic kidneys over a 16-week period [19]. Both males and female animals were included in this study, however, due to gender dimorphism in this model (males having higher cystic burden), the majority of subsequent analyses was only conducted in males [19]. Genotyping of *jck* mice was performed using genomic DNA obtained from ear punch material using Extract-N-Amp^{TM} Tissue PCR Kit (Sigma-Aldrich, St. Louis MO, USA). PCR was carried out on this genomic material using primers IMR4004 (CTT CCC ACC TGT TGC TGT TT) and IMR4005 (CAG TGG GCT TAC CAC CAT CT) for 30 cycles at 55 °C [15]. The resultant PCR product was digested with BseY1 (New England Biolabs, Ipswich MA, USA), and the digested product was electrophoresed on 2% agarose gel to separate the products and identify genotypes. The mutant gene produced a band of 300 base pairs, while the wild-type gene produced two bands at 200 and 100 base pairs (see Supplementary Data, Fig. S1).

jck/Cdk2$^{-/-}$ C57BL/6J compound mice

To produce the compound mice, a two-step process was required, as homozygous *Cdk2* knockout animals are sterile due to small gonads [8]. *Cdk2* mice were generated in the Kaldis Laboratory (Institute of Molecular and Cell Biology (IMCB), Singapore) [8], and breeding pairs were imported and maintained in the Westmead Hospital Animal Facility. Heterozygous *jck* mice were mated with heterozygous *Cdk2* mice. Both were on a C57BL/6J background. Progeny with the correct genotype (*Nek8*$^{jck/-}$*/Cdk2*$^{+/-}$) were then mated to produce *jck/Cdk2*$^{-/-}$ mice. Animals with the desired genotype were predicted to be 6.25% of the animals produced, however, the actual rate was much lower. Genotyping of mice was performed using the same method described above. *Cdk2* PCR was performed under similar conditions as with the *jck* gene. The three primers used were PKO0292 (GTG ACC CTG TGG TAC CGA GCA CCT G), PKO0294 (CCC GTG ATA TTG CTG AAG AGC TTG GCG G), and PKO0344 (GGT TTT GCT CTT GGA TGT GGG CAT GG) [8]. Annealing temperature was 60 °C for 30 cycles. The Neomycin gene produced a band of 500 base pairs, while the wild-type gene was a 150 base pair band. Genotyping was performed for all animals and confirmed the absence of *Cdk2* (see Supplementary Data, Fig. S1).

All studies were approved by the Westmead Hospital Institutional Animal Care and Use Committee (Protocol No. 1014.02-08). Animals were allowed ad libitum access to standard chow and water.

Experimental design

Three studies were undertaken: (i) Study 1: to determine the kinetics of cell proliferation and cell-cycle regulatory proteins, a time course study was performed. Groups of *jck* mice were sacrificed on day 28, day 56, and day 84 ($n = 6$ male, $n = 6$ female per timepoint) and compared with age-matched wild-type animals ($n = 4$ male, $n = 4$ female per timepoint); (ii) Study 2: to determine the effect of *Cdk2* deficiency on the progression of *jck* mice, compound *jck/Cdk2*$^{-/-}$ mice ($n = 6$ male, $n = 5$ female) were sacrificed at day 84, and compared with age-matched *jck/ Cdk2*$^{+/+}$ ($n = 6$ male, $n = 6$ female) and wild-type mice ($n = 4$ male, $n = 4$ female); (iii) Study 3: to determine the effects of sirolimus on cell-cycle-associated proteins in *jck* mice, groups of *jck* mice ($n = 6$ male, $n = 6$ female per group) were treated with either vehicle (90% saline, 10% ethanol) or sirolimus (0.5 or 1 mg/kg body weight/day) by daily injection from postnatal day 28, and then sacrificed on day 43. The dosages, route of administration and length of treatment were determined based on previous studies [19, 20].

At the time of sacrifice, mice were anaesthetized with ketamine: xylazine, blood was collected by cardiac puncture, and kidneys were removed and weighed. Two kidney weight to body weight ratio (KW: BW) was calculated by the following formula: (*left kidney weight + right kidney weight/ total body weight*). Tissues were fixed in either 10% neutral buffered formalin or methyl Carnoy's solution for 24 h, then paraffin-embedded, or snap-frozen in liquid nitrogen.

Assessment of disease progression and renal function

Sections (4 μm thick) were cut from the paraffin blocks and stained by Periodic Acid Schiff (PAS) stain, or 0.1% sirius red, and 0.1% fast green in picric acid stain, to assess cyst area and interstitial fibrosis, respectively. Kidney cyst volume was calculated using digital whole-slide images with the Optimas image analyses software (Adept Turnkey, Sydney NSW, Australia). Serum extracted from blood collected at the time of sacrifice was analyzed for creatinine and urea at the Institute of Clinical Pathology and Medical Research (Westmead Hospital, Sydney NSW, Australia).

Immunohistochemistry

Sections (4 μm thickness) were deparaffinized in Histoclear (Fronine, Sydney NSW, Australia) and rehydrated through a series of graded alcohols. Endogenous peroxidase was blocked using 3% hydrogen peroxide in methanol for 8 min. Nonspecific binding was blocked using Background Buster (Innovex Biosciences, Richmond VA, USA). For formalin-fixed sections, heat induced antigen retrieval was performed by microwave oven heating in 1x Antigen Decloaker (Biocare, Pacheco CA, USA). The primary antibodies used were: anti-Ki-67 (1:200; Neomarkers, Fremont CA, USA), anti-bromodeoxyuridine (BrdU) (1:100, Novus Biologicals, Littleton CO, USA), anti-F4/80 (1:100; Serotec, Hercules CA, USA), anti-alpha smooth muscle actin (α-SMA) (1:4000; Sigma-Aldrich), anti-cyclin D1 (1:50; Neomarkers), anti-cyclin A (1:100; Cell Signaling Technology, Danvers MA, USA), anti-pRb (Ser 780) (1: 250; Cell Signaling Technology), anti-vimentin (clone V9) (1:100; Dako Agilent Technologies, Santa Clara CA, USA), anti-histone H2A.X (1:2000; Abcam, Cambridge, U.K.), and anti-phospho-histone H2A.X (Ser139) (1:480; Cell Signaling Technology). Immunohistochemistry was also performed using the following primary antibodies to determine cyst origin: anti-aquaporin-1 (1:200; Abcam; proximal tubules and descending loop of Henle), anti-aquaporin-2 (1:200; Abcam; collecting duct), anti-Tamm Horsfall Glycoprotein (1:400; ascending loop of Henle). Antibodies were diluted in DaVinci Green diluent (Biocare) and sections were incubated for 1 h at room temperature or overnight at 4 °C. After washing with PBS, slides were incubated with the appropriate biotinylated secondary antibody for 30 min at room temperature. The signal was amplified using Vectastain R.T.U. ABC reagent (Vector Laboratories, Burlingame CA, USA) and visualized with diaminobenzidine. The slides were counterstained with methyl green or haematoxylin. The sections were dehydrated through a series of graded alcohols and permanently mounted in Vectamount (Vector Laboratories). Slides were scanned using Scanscope CS2 (Leica Microsystems, Sydney NSW, Australia) or NanoZoomer v1 (Hamamatsu Photonics, Japan) for digital whole-slide images. Aperio Imagescope (v11.2.0.780, Leica Biosystems, Wetzlar, Germany) was used to analyze the images for positive staining. For the quantification of percentage positive Ki-67 cells by cyst size in *jck* mice, the circumference of randomly chosen cysts were measured and allocated into a category of small, medium or large: small cysts had <10 CECs per cyst and circumference of <250 μm, medium cysts had approximately 10–30 CECs per cyst with circumference ranging from 250–750 μm, and large cysts had >30 CECs per cyst and circumference >750 μm.

Western blot

Protein samples were prepared from kidney tissue samples using radioimmunoprecipitation assay (RIPA) buffer with protease inhibitors (Roche, Basel, Switzerland) and phosphatase inhibitors (ThermoFisher Scientific, Waltham, USA). The tissue was mechanically disrupted using a Dounce homogenizer. After spinning for 15 min at 12,000 rpm, samples were stored at −80 °C until required. The DC Protein Assay (Bio-Rad, Hercules CA, USA) was performed, and 100 μg of lysate was loaded onto a 4–12% Bis-Tris acrylamide gel (Invitrogen, Waltham MA, USA) or a 4–15% Mini-Protean® TGX Stain-Free™ Precast Gel (Bio-Rad, Hercules CA, USA) and run for 60 min at 200 V under reducing conditions. The gel was transferred to a nitrocellulose or PVDF membrane using iBlot (Invitrogen) or wet transfer and blocked overnight with 50% Odyssey Blocking buffer (LI-COR Biosciences, Lincoln NE, USA) or 3% bovine serum albumin. The membrane was probed with antibodies against cyclin D1 (1:100; Neomarkers), cyclin E (1:500; Cell Signaling Technology), cyclin A (1:1000; Santa Cruz Biotechnology, Dallas TX, USA), cyclin B1 (1:500; Cell Signaling Technology), pRb (Ser 780) (1:250; Cell Signaling Technology), Rb (1:5000; Santa Cruz Biotechnology), *Cdk5* (1:1000; Cell Signaling Technology), and GAPDH (1:2000; Abcam), overnight at 4 °C. After washing, blots were incubated with the appropriate infrared fluorescent-conjugated secondary antibodies. The blots were scanned on the Odyssey Imaging System (LI-COR Biosciences) at 700 and 800 nm. The resultant scans were normalized to GAPDH or total protein using Image J software (v1.47, National Institutes of Health, USA) and ImageLab™ Software (v6.0.1, Bio-Rad).

Immunoprecipitations and kinase assays

Affinity purification, immunoprecipitations, and kinase assays were performed as described previously [8], with minor modifications. Briefly, 50–250 μg of protein extract was incubated with proteins/antibodies that were either

covalently conjugated to agarose beads (for *Cdk2* [8], cyclin B1 [Santa Cruz, sc-7393], cyclin A2 [Santa Cruz, sc-751]), or unconjugated (for *Cdk1*, [Santa Cruz, sc-954]). Unconjugated antibodies together with bound proteins were isolated the following day by incubation for 1 h with protein A agarose beads (Roche, 11719408001). After four washes in EBN buffer and one wash in EB buffer (EBN without NP-40), the precipitated proteins were either resolved by SDS-PAGE for western blot analysis or used in kinase assays to determine the levels of enzyme activity against the substrate histone H1 (Roche, 11004875001). Kinase assays were performed by incubating the immunoprecipitated, bead-bound proteins in EB buffer supplemented with 10 mM DTT, 15 µM ATP, 5 µCi [ϒ-P^{32}]ATP (PerkinElmer, NEG502A, Waltham MA, USA), and 1.5 µg histone H1 for 30 min at room temperature. The assay mixture was then inactivated in SDS-PAGE sample buffer and subjected to electrophoresis on polyacrylamide gel, then fixed and stained in Bismarck Brown/Coomassie blue prior to the quantification of incorporated radioactivity using a PhosphoImager (Fujifilm, FLA-7000).

Statistics

Data were expressed as means ± SD. Data was analyzed using JMP® Student Edition statistical software package (v12.1.0, SAS Institute, Cary NC, USA). A P value < 0.05 was considered statistically significant. Differences between groups were examined using a one-way analysis of variance (ANOVA), followed by the non-parametric, 2-sample Mann–Whitney U test, or parametric, independent-samples t-test.

Results

Characteristics of jck mice

To understand the phenotype of *jck* mice, we analyzed their appearance, body weight, and kidney size. The appearance of *jck* mice was similar to wild-type mice. Body weight increased steadily in both groups, but *jck* mice weighed less than wild-type mice at day 28 and day 84 (Table 1). Kidneys from *jck* mice increased in size and macroscopically appeared cystic from day 28 onward. The kidney enlargement, as assessed by KW: BW, was 1.7, 2.7-, and 5.6-fold higher than wild-type mice at day 28, day 56, and day 84, respectively (Table 1). Female *jck* mice weighed less than male *jck* mice on day 56 and 84, however, kidney enlargement was comparable (see Supplementary Data, Table S1). The onset of kidney enlargement at day 28 in *jck* mice, preceded the development of renal dysfunction, as assessed by the serum creatinine and urea (Table 1). However, there was large variation in serum urea and creatinine for *jck* mice, and therefore, results were not statistically different between groups. Heart to body weight ratio (HW: BW) was increased in *jck* mice (Table 1).

Table 1 Physical and biochemical parameters in male and female wild-type and juvenile cystic kidney (*jck*) mice on day 28, 56, and 84.

Parameter	Type	Age (Days)		
		28	56	84
Body weight (g)	wt	14 ± 2	19 ± 1	25 ± 4
	jck	11 ± 2[a]	21 ± 4	21 ± 4[a]
Right kidney weight (g)	wt	0.07 ± 0.01	0.10 ± 0.01	0.16 ± 0.04
	jck	0.10 ± 0.02	0.33 ± 0.13[a]	0.65 ± 0.20[a]
Left kidney weight (g)	wt	0.08 ± 0.01	0.11 ± 0.01	0.15 ± 0.05
	jck	0.11 ± 0.04[a]	0.31 ± 0.10[a]	0.70 ± 0.23[a]
KW: BW (%)	wt	1.09 ± 0.13	1.12 ± 0.07	1.19 ± 0.25
	jck	1.86 ± 0.23[a]	3.02 ± 0.68[a]	6.71 ± 2.69[a]
HW: BW (%)	wt	0.55 ± 0.06	0.51 ± 0.05	0.50 ± 0.09
	jck	0.53 ± 0.09	0.54 ± 0.10	0.63 ± 0.13[a]
Serum urea (mmol/L)	wt	6.37 ± 2.06	7.37 ± 0.12	6.60 ± 2.48
	jck	4.40 ± 1.04	7.17 ± 2.10	34.60 ± 16.54
Serum creatinine (µmol/L)	wt	17.63 ± 2.10	17.33 ± 0.58	16.60 ± 4.41
	jck	18.00 ± 4.00	19.33 ± 1.15	52.67 ± 25.70

Data expressed as mean ± SD

KW kidney weight, *BW* body weight, *HW* heart weight, *D* day, *wt* wild-type, *jck* juvenile cystic kidney

[a]$P < 0.05$ by the 2-sample Mann–Whitney U test compared with age-matched wild-type animals

By light microscopy, focal renal cyst formation was detected from day 28 and cyst area increased by day 84 in *jck* mice (Fig. 2a, b). Total renal cell proliferation, as assessed by Ki-67 immunostaining, was increased in *jck* mice compared with wild-type animals, peaking on day 56 (Fig. 3a). When comparing proliferation in cystic and noncystic renal tissue in *jck* mice, proliferation peaked on day 56 for the former, and day 28 for the latter (Fig. 3b). In addition, when grouped by renal cyst size (small, medium, large), the number of positive Ki-67 proliferation was highest on day 28 (Fig. 3c). Taken together, these data suggest that cystic epithelial cell proliferation peaks during the early-mid phases of the model.

Tubulointerstitial disease increased progressively in *jck* mice, peaking on day 84 (Fig. 4). The number of interstitial monocytes, as assessed by the number of F4/80-positive cells, increased significantly around renal cysts from day 28 to day 84 (Fig. 4a). Monocytes were recruited to the interstitium around CECs and were increased at day 56 and 84 in *jck* mice (Fig. 4a). Similarly, peri-cystic and interstitial myofibroblast accumulation, as assessed by the number of

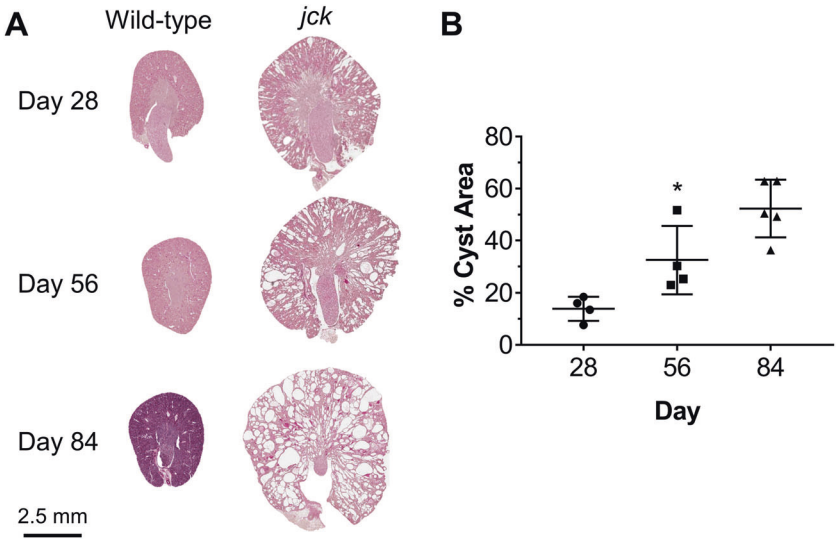

Fig. 2 Progression of cystic renal disease in male wild-type (wt) and juvenile cystic kidney (*jck*) disease mice on day 28, 56, and 84. a Representative whole-slide digital images of Periodic Acid Schiff (PAS)-stained sections from male wt and *jck* mice on day 28, 56, and 84. Scale bar = 2.5 mm. **b** Percentage cyst area in male *jck* mice at day 28, 56, and 84. $*P < 0.05$ by 2-sample Mann–Whitney *U* test when compared with day 28 *jck* mice. wt wild-type, *jck* juvenile cystic kidney.

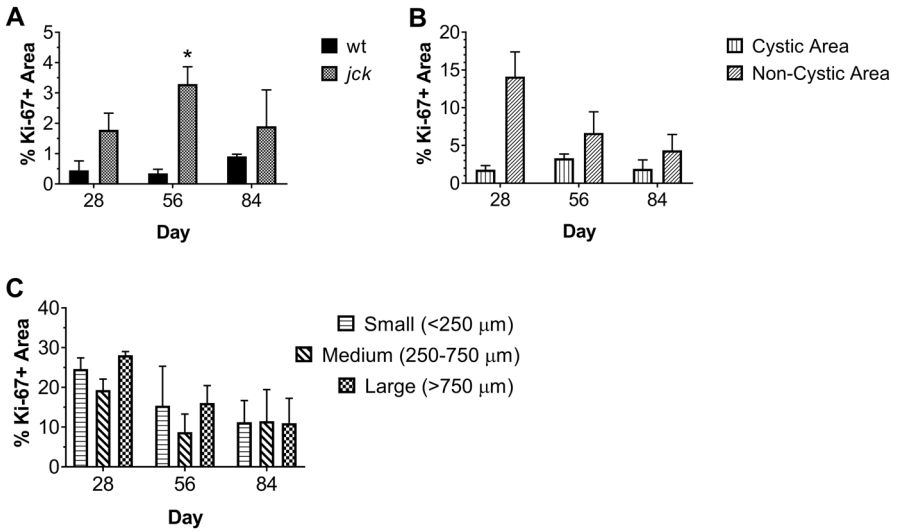

Fig. 3 Renal cell proliferation in male wild-type (wt) and juvenile cystic kidney (*jck*) disease mice, assessed by immunohistochemistry using Ki-67, on day 28, 56, and 84. a Percentage Ki-67 positive staining area in the total coronal kidney area for male wt and *jck* mice on day 28, 56, and 84. **b** Percentage Ki-67 positive staining area according to cystic and noncystic area in *jck* mice on day 28, 56, and 84. **c** Ki-67 positive cells as a percentage of total cells according to cyst size in *jck* mice on day 28, 56, and 84. Small cysts had <10 cystic epithelial cells (CECs) per cyst and circumference of <250 μm. Medium cysts had ~10–30 CECs per cyst and circumference ranged from 250–750 μm. Large cysts had >30 CECs per cyst and circumference was >750 μm. $*P < 0.05$ by 2-sample Mann–Whitney *U* test compared with age-matched wild-type mice. wt wild-type, *jck* juvenile cystic kidney.

α-SMA-positive cells, also increased, peaking on day 84 (Fig. 4b). Myofibroblasts were present at all timepoints but increased at 56 and 84 in *jck* mice. No CECs were found to be positive for α-SMA. There was little deposition of interstitial collagen in *jck* mice (<1% of total area), and this was not statistically different to wild-type mice (Fig. 4c). Other markers of epithelial cell dedifferentiation (vimentin and E-cadherin) were also examined by western blot of whole kidney protein extracts. Vimentin expression was increased in *jck* mice compared with wild-type mice from day 56 onward (see Supplementary Data, Fig. S2a), whereas the renal expression of E-cadherin was not altered (see Supplementary Data, Fig. S2b).

Kinetics of Cdk2 and Cdk2-cyclin partners in jck mice

The activation of Cdks in the cell-cycle progression is dependent on the expression of specific cyclins that are upregulated during defined stages [6]. To first understand the importance of *Cdk2* in relation to disease progression, we assessed the expression of its cyclin partners, cyclin A and E, in *jck* mice over time. Using the western blot analysis

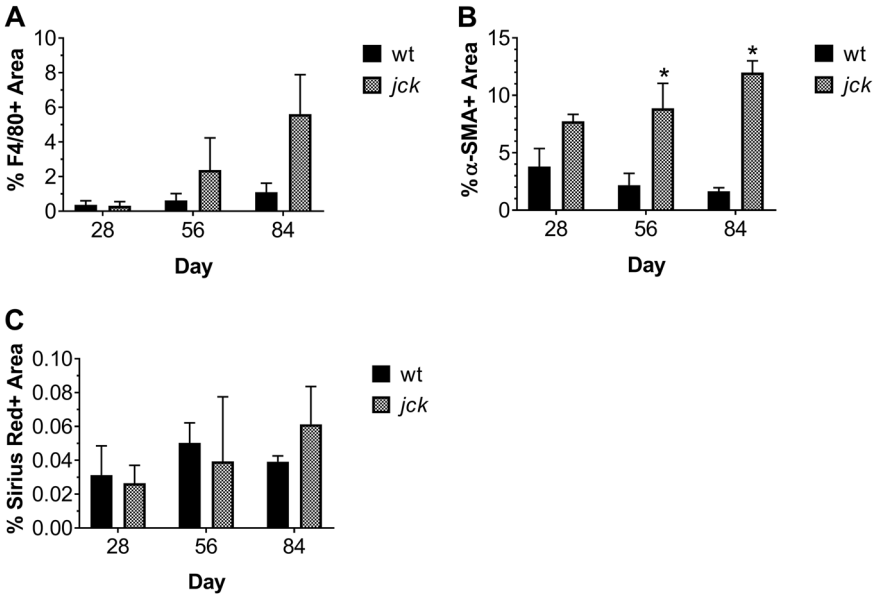

Fig. 4 Histological markers of kidney disease progression in male wild-type (wt) and juvenile cystic kidney (*jck*) disease mice on day 28, 56, and 84. a Percentage of F4/80 positive staining area, as a measure of interstitial monocyte accumulation. **b** Percentage of α-smooth muscle actin (α-SMA) positive staining area, as a measure of myofibroblast infiltration. **c** Percentage of sirius red positive staining area, as a measure of fibrosis. *$P <$ 0.05 by 2-sample Mann–Whitney *U* test compared with age-matched wild-type mice. wt wild-type, *jck* juvenile cystic kidney.

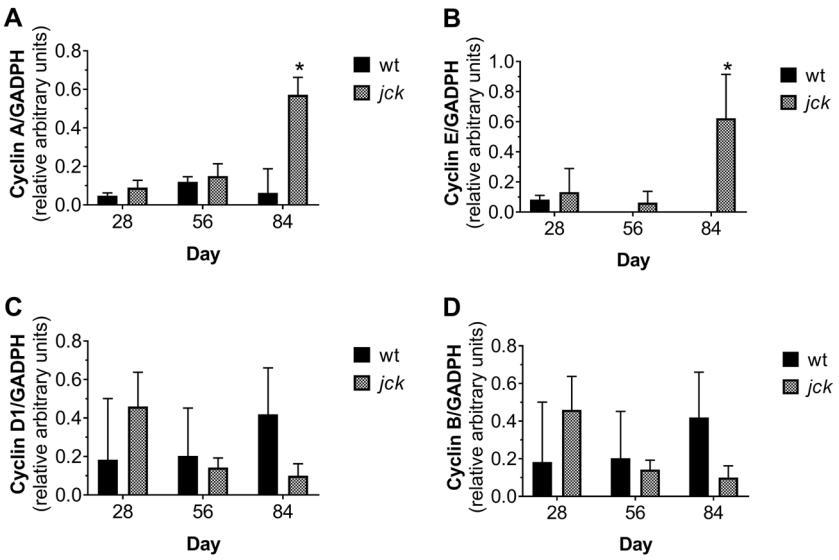

Fig. 5 Relative expression of cyclins measured by western blot using nuclear extracts from whole kidney tissues in male wild-type (wt) and juvenile cystic kidney (*jck*) disease mice on day 28, 56 and 84. Relative **a** cyclin A, **b** cyclin E, **c** cyclin D1 and **d** cyclin B protein expression. GAPDH was used as the loading control. *$P < 0.05$ by 2-sample Mann–Whitney *U* test compared with age-matched wild-type mice. wt wild-type, *jck* juvenile cystic kidney.

of whole kidney nuclear extracts, the expression of cyclins E and A increased on day 84 in *jck* compared with wild-type (Fig. 5a, b). In contrast, cyclin B and D1 expression did not differ significantly between *jck* and wild-type mice at any timepoints (Fig. 5c, d). By immunohistochemistry, cyclin D1 was localized to CECs and was significantly higher in *jck* mice on day 28 and 84, compared with wild-type mice (Fig. 6a, c). In contrast, cyclin A was found in peritubular spindle-shaped cells and the expression peaked at day 84, consistent with western blot data (Fig. 6b, c). pRb protein was only detectable at day 84 in *jck* mice, and not at other timepoints (Fig. 7b). Since the assessment of cyclin protein by western does not allow determination of the kinase activity, we measured *Cdk1* and *Cdk2* by the H1 assays where the band intensity is directly proportional to kinase activity. As shown in Fig. 8, kinase activity for *Cdk1*, *Cdk2*, and its partner cyclin A2 were increased at later timepoints (days 56 and 84) in *jck* mice.

Effect of Cdk2 deficiency on renal disease progression in jck mice

As expected, both wild-type and compound mice with *Cdk2* deficiency had reduced gonad size and infertility (Fig. 9a) [8], but no effect on body weight was observed (Table 2). The absence of *Cdk2* did not alter the development of kidney enlargement and renal dysfunction in *jck* mice, as no significant differences were found when compared with *jck* mice (Table 2). This result was consistent when sub-analyzed by gender (see Supplementary Data, Table S2). By

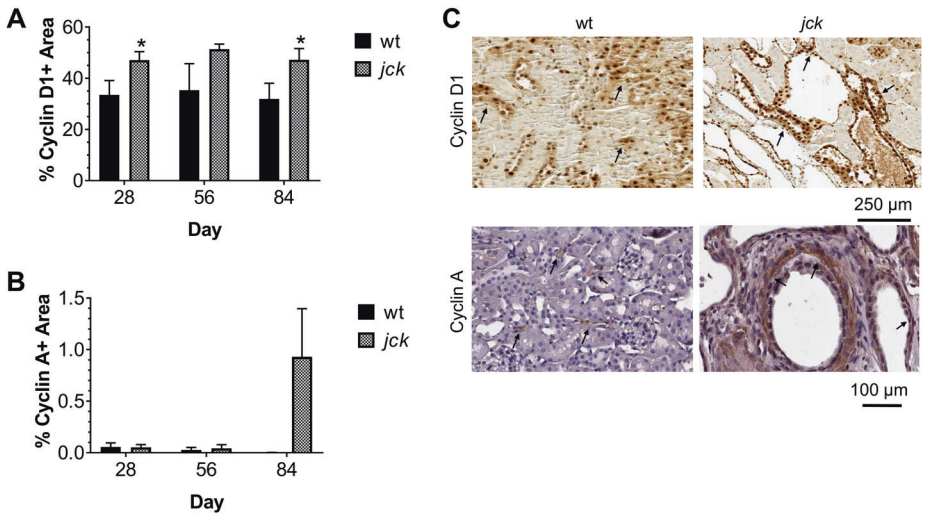

Fig. 6 Expression of cyclins measured by immunohistochemistry in kidney tissue of male wild-type (wt) and juvenile cystic kidney (*jck*) disease mice on day 28, 56, and 84. a Percentage of cyclin D1 positive staining area. **b** Percentage of cyclin A positive staining area. **c** Representative images of cyclin D1 and A-stained kidney sections from male wt and *jck* mice on day 56. Magnification is ×10 for cyclin D1 and ×20 for cyclin A. Scale bar = 250/100 µm, respectively. $*P < 0.05$ by 2-sample Mann–Whitney *U* test compared with age-matched wild-type mice. wt wild-type, *jck* juvenile cystic kidney.

histological analysis, the progression of cystic renal disease was similar in *jck/Cdk2*$^{+/+}$ mice compared with the *jck/Cdk2*$^{-/-}$ mice, as assessed by percentage cyst area, number of cysts, renal cell proliferation, interstitial collagen, monocyte, and myofibroblast accumulation (Figs. 9b–d and 10). Furthermore, the nephron-segment origin of cysts was also the same in both groups (Fig. 11).

Persistent upregulation of Cdk1 in Cdk2-deficient jck mice

Since proliferation, as determined by BrdU incorporation, was similar in the presence or absence of *Cdk2* (Fig. 10a), we evaluated the potential mechanisms underlying the failure of *Cdk2* deficiency to alter disease progression. Therefore, the activity of *Cdk1*, *Cdk2,* and their cyclin partners in *jck/Cdk2*$^{+/+}$ mice and *jck/Cdk2*$^{-/-}$ mice was assessed. In Fig. 12, background levels of *Cdk2* activity were observed in *jck/Cdk2*$^{-/-}$ mice, whereas the western blot analysis of the immunoprecipitate showed no band, confirming that *Cdk2* protein was not present. The discrepancy between the *Cdk2* activity in the kinase assay and the Cdk2 protein in the western blot analysis can be attributed to: (i) non-specific background; (ii) sample contamination (that is, lack of specificity from the Cdk2 antibody may have caused other Cdks or non-specific kinases to be immunoprecipitated, resulting in detected activity); and/or (iii) a false positive result due to overexposure of the gel to X-ray film [21].

As shown in Fig. 12, *Cdk1*, cyclin B2, and cyclin A2 activity was persistent and higher in *jck/Cdk2*$^{-/-}$ mice compared with *jck/Cdk2*$^{+/+}$ mice, potentially explaining the increase in proliferation and BrdU incorporation observed in Fig. 10a. To determine whether *Cdk1* was involved in cell proliferation in this disease model, we treated *jck* mice with sirolimus (an anti-proliferative agent). Sirolimus treatment resulted in reductions in body weight, kidney enlargement, phosphorylated S6, CEC proliferation, and phosphorylated Rb (Figs. 13, 14). In addition, treatment with sirolimus was also associated with reduced *Cdk1*, *Cdk2*, cyclin A2, and cyclin B1 activity in *jck/Cdk2*$^{+/+}$ mice in a dose-dependent manner (Fig. 12).

A key role for *Cdk2* is mediating the transition from G_1 to S phase, which requires passing the G_1/S DNA damage checkpoint [6]. Satyanarayana et al. [22] demonstrated *Cdk2*$^{-/-}$ mice had increased sensitivity to irradiation, and exhibited delayed continuation of DNA replication. Furthermore, recent studies suggest a link between DNA damage and kidney cyst formation in PKD [23–25]. Therefore, markers of DNA damage, H2AX and its phosphorylated form (γ-H2AX), were also assessed. H2AX was diffusely expressed in most nuclei for both wild-type and *jck* mice, but stronger staining was observed in distal tubular structures and CECs of both *jck/Cdk2*$^{+/+}$ and *jck/Cdk2*$^{-/-}$ mice (see Supplementary Data, Fig. S3). In addition, γ-H2AX nuclear expression was increased in both *jck/Cdk2*$^{+/+}$ and *jck/Cdk2*$^{-/-}$ mice compared with wild-type, and localized to cystic tubules (see Supplementary Data, Fig. S4). However, no differences in H2AX or γ-H2AX expression were observed in *Cdk2*$^{-/-}$ tissue compared with *Cdk2*$^{+/+}$ tissue for both wild-type and *jck* mice (see Supplementary Data, Figs. S3–4).

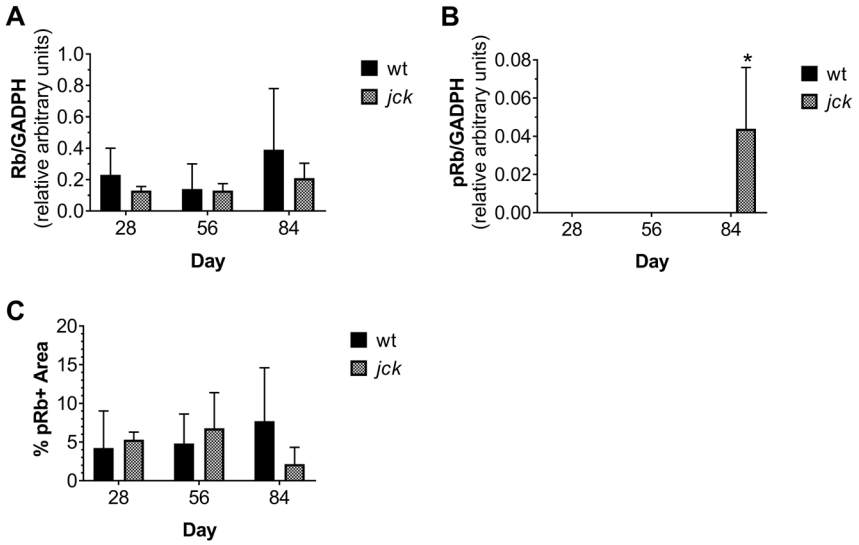

Fig. 7 Expression of retinoblastoma (Rb) protein and its phosphorylated form (pRb), measured by western blot and immunohistochemistry, in male wild-type (wt) and juvenile cystic kidney (*jck*) disease mice on day 28, 56, and 84. a Relative Rb protein expression by western blot. **b** Relative pRb protein expression by western blot. **c** Percentage pRb positive staining area by immunohistochemistry. GAPDH was used as the loading control. $*P < 0.05$ by 2-sample Mann–Whitney *U* test compared with age-matched wild-type mice. wt wild-type, *jck* juvenile cystic kidney.

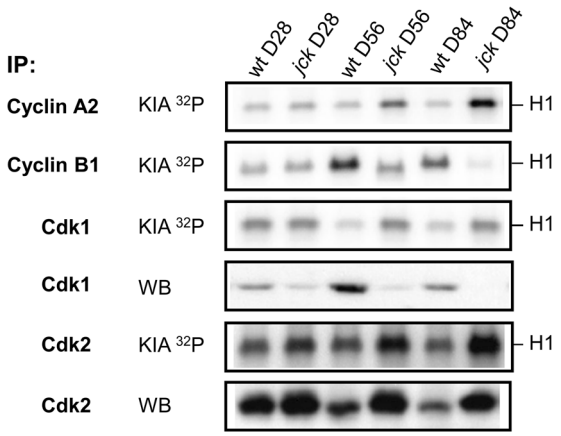

Fig. 8 The histone H1-kinase activity and western blot analysis of immunoprecipitated cyclins and cyclin-dependent kinases (Cdks) from male wild-type (wt) and juvenile cystic kidney (*jck*) disease mice on day 28, 56, and 84. IP immunoprecipitation, KIA kinase assay, WB western blot, D day, wt wild-type, *jck* juvenile cystic kidney, *Cdk* cyclin-dependent kinase. H1 histone H1.

Persistent cystic disease in the absence of Cdk2 is unlikely due to Cdk5 activity

Husson et al. [10] recently demonstrated a role for *Cdk5* in regulating ciliary length and epithelial cell differentiation in *jck* mice. Therefore, we assessed the expression of *Cdk5* using western blot in the current study. As shown in Fig. 15b, the renal expression of *Cdk5* expression was increased in *jck/Cdk2*$^{+/+}$ mice, compared with wild-type/*Cdk2*$^{+/+}$ mice. There was no difference in *Cdk5* expression between wild-type/*Cdk2*$^{+/+}$ and wild-type/*Cdk2*$^{-/-}$. In contrast, *Cdk5* expression was reduced by the absence of Cdk2 in *jck* mice (Fig. 15b). To determine if the reduction in renal *Cdk5* in the *jck/Cdk2*$^{-/-}$ mice had a functional impact of epithelial cell differentiation, we further evaluated the expression of vimentin. However, as shown in Supplementary Data, Fig. S2c, qualitative analysis demonstrated that tubular vimentin expression was increased in *jck* mice but not altered by the absence of *Cdk2*.

Discussion

Targeting Cdks has been hypothesized to reduce CEC proliferation, cyst enlargement, and kidney failure due to PKD [10, 13, 14]. In the past decade, research relating to the pharmacological inhibition of Cdks (such as roscovitine) has demonstrated promising therapeutic potential in PKD, by attenuating cyst growth and improving renal function [13, 14]. However, the in vivo role of specific G_1-phase Cdks in the progression of PKD has not been explored.

This study assessed the role of *Cdk2* deficiency in the preclinical *jck* mouse model. The main finding of the study was that *Cdk2* was dispensable in PKD progression, as *Cdk2* deficiency from birth had no effect on cyst growth, proliferation, fibrosis, inflammation, or renal function decline. The kinase assay revealed that *Cdk2* activity was upregulated in *jck* mice compared with wild-type animals, and peaks at later timepoints (days 56–84). Furthermore, the expression of the cyclin partners of *Cdk2* (cyclin A and E)

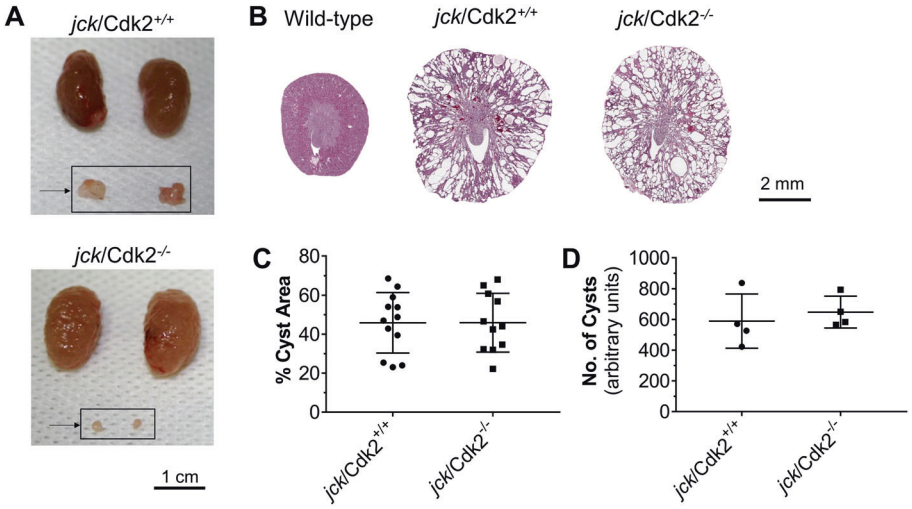

Fig. 9 Progression of cystic renal disease in male and female juvenile cystic kidney (jck) disease mice in the absence or presence of cyclin-dependent kinase 2 (*Cdk2*) on day 84. a Representative photographs of polycystic kidneys and ovaries from female *jck*/Cdk2$^{+/+}$ (top) and *jck*/Cdk2$^{-/-}$ (bottom) mice. Scale bar = 1 cm. **b** Representative whole-slide digital images of Periodic Acid Schiff (PAS)-stained sections from wt, *jck*/Cdk2$^{+/+}$ and *jck*/Cdk2$^{-/-}$ mice. Scale bar = 2 mm. **c** Percentage cyst area in *jck*/Cdk2$^{+/+}$ and *jck*/Cdk2$^{-/-}$ mice. **d** Number of cysts in *jck*/Cdk2$^{+/+}$ and *jck*/Cdk2$^{-/-}$ mice. wt wild-type, *jck* juvenile cystic kidney, *Cdk* cyclin-dependent kinase.

Table 2 Physical and biochemical parameters of male and female wild-type and juvenile cystic kidney (*jck*) disease mice with or without *Cdk2* ablation from birth on day 84.

Parameter	wt/Cdk2$^{+/+}$	wt/Cdk2$^{-/-}$	*jck*/ Cdk2$^{+/+}$	*jck*/Cdk2$^{-/-}$
Body weight (g)	22 ± 3	22 ± 4	23 ± 4	21 ± 3
Right kidney weight (g)	0.15 ± 0.03	0.13 ± 0.03	0.74 ± 0.47[a]	0.69 ± 0.50[a]
Left kidney weight (g)	0.15 ± 0.03	0.12 ± 0.02	0.74 ± 0.50[a]	0.66 ± 0.46[a]
KW: BW (%)	0.67 ± 0.07	0.56 ± 0.05[a]	3.52 ± 2.88[a]	3.45 ± 2.99[a]
HW: BW (%)	0.52 ± 0.08	0.45 ± 0.05	0.61 ± 0.20	0.55 ± 0.12
Serum urea (mmol/L)	7.04 ± 1.64	7.73 ± 2.75	27.37 ± 41.19[a]	30.11 ± 35.40[a]
Serum creatinine (μmol/L)	16.13 ± 4.79	17.14 ± 6.44	27.75 ± 19.41	33.92 ± 23.00[a]

Data expressed as mean ± SD

wt wild-type, *Cdk* cyclin-dependent kinase, *KW* kidney weight, *HW* heart weight, *BW* body weight, *jck* juvenile cystic kidney

[a]$P < 0.05$ by the 2-sample Mann–Whitney *U* test compared with age-matched wild-type animals

was increased on day 84, and accompanied by increased expression of pRb, a downstream target of *Cdk2*, indicating a potential role in disease progression. However, the peak expression of *Cdk2*, its cyclin partners and pRb at days 56–84, did not correlate with trends in proliferation, which appeared to be greatest much earlier in the disease model at days 28–56. Similar to the phenotype reported in previous studies, *Cdk2*$^{-/-}$ mice had reduced gonad size [8]. The activity of both *Cdk1* and its partner cyclin, cyclin B1, was higher in *jck/Cdk2*$^{-/-}$ mice compared with *jck/Cdk2*$^{+/+}$ mice, and the functional significance of *Cdk1* in disease progression was further confirmed by its downregulation in response to treatment with an antiproliferative agent (sirolimus). Therefore, in the absence of *Cdk2*, higher *Cdk1* activity likely plays a compensatory role, allowing continual cell-cycle progression, proliferation of CECs, and PKD progression.

Interestingly, our study demonstrated that the timing of peak expression for *Cdk2*, its cyclin partners, and pRb did not correlate with the timing of peak expression for the proliferative marker, Ki-67. One possible reason is that transient changes in Cdks and their associated cyclin activity occur prior to day 28 or between day 28 and 56, which were not assessed in this present study. However, contrary to our study, previous studies in *jck* mice have suggested that the activity of Cdks at later timepoints is associated with proliferation of CECs, as roscovitine (a pan-Cdk inhibitor) was effective in attenuating progression of cystic disease when administered from day 26 [13]. In the *jck* mouse, the trends in proliferation differed significantly between cystic and noncystic tissue, where the highest levels of proliferation were observed in noncystic renal cells at day 28. This may be attributed to rapidly proliferating

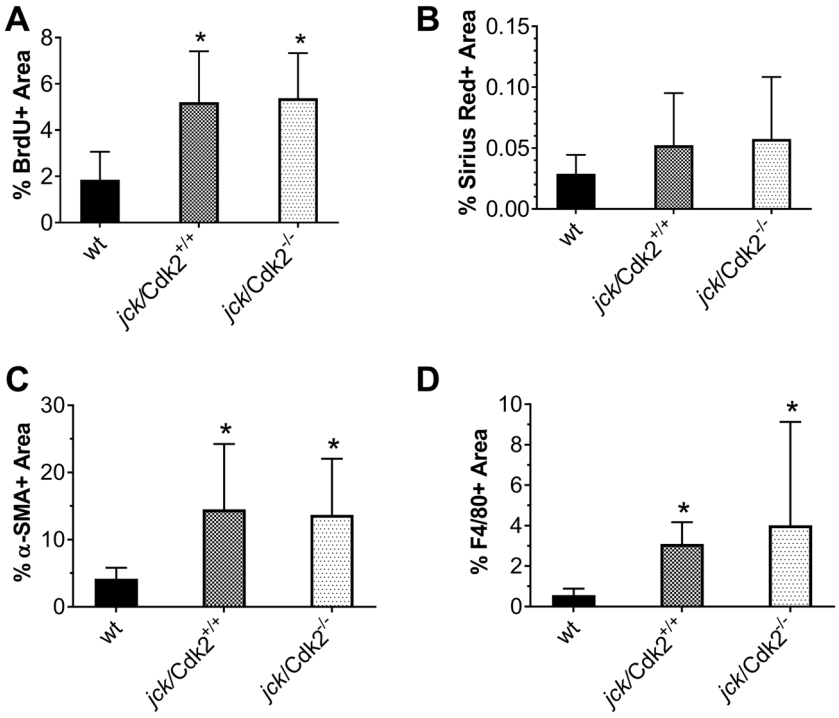

Fig. 10 Histological markers of kidney disease progression in male and female wild-type (wt) and juvenile cystic kidney (*jck*) disease mice in the absence or presence of cyclin-dependent kinase 2 (*Cdk2*) on day 84. a Percentage of bromodeoxyuridine (BrdU) positive staining area, as a measure of renal cell proliferation. **b** Percentage of sirius red positive staining area, as a measure of fibrosis. **c** Percentage of F4/80 positive staining area, as a measure of interstitial monocyte accumulation. **d** Percentage of α-smooth muscle actin (α-SMA) positive staining area, as a measure of myofibroblast infiltration. $*P < 0.05$ for comparisons to wild-type animals, $P < 0.05$ for comparisons between *jck* and *jck*/Cdk2$^{-/-}$ mice by 2-sample Mann–Whitney *U* test. BrdU bromodeoxyuridine, wt wild-type, *jck* juvenile cystic kidney, *Cdk* cyclin-dependent kinase.

epithelial cells that have yet to become cystic in phenotype. Therefore, another possible explanation for this lack of correlation is the use of whole kidney extracts to examine *Cdk* and cyclin expression, rather than isolating cystic tissue from noncystic tissue to be analyzed separately.

The most likely explanation for the lack of effect of *Cdk2* deficiency on PKD progression is due to compensation from other Cdks, namely *Cdk1*, which normally forms complexes with both cyclin A and B, and plays a significant role in mitosis (Fig. 1). The compensatory ability for *Cdk1* was first demonstrated in vivo, where *Cdk1* was able to bind and interact with cyclin E1 in the absence of *Cdk2* [26]. This observation was further established by Santamaría et al. [27], who demonstrated that mouse embryos with triple knockout of *Cdk4*, *Cdk6,* and *Cdk2* still underwent morphogenesis, organogenesis, and development until embryonic day 12.5. This triple knockout study demonstrated that most cells continued to proliferate, evidenced by Ki-67 expression, and most primary mouse embryonic fibroblast cultures became immortal upon continuous passage [27], emphasizing that *Cdk1* alone may be adequate to drive mammalian cell cycle. It is also confirmed that *Cdk1* is able to bind and interact with other non-partner cyclins, including D1, D2, and E [27–29]. In addition, though H2AX and γ-H2AX expression was increased in *jck* mouse kidneys compared with wild-type (consistent with findings by Choi et al. [23]), no differences in DNA damage were observed between *Cdk2*$^{+/+}$ and *Cdk2*$^{-/-}$ mice. These data suggest that G_1/S phase DNA damage checkpoint function was not altered by the absence of *Cdk2*. Therefore, we hypothesize that *Cdk1* activity was upregulated in the absence of *Cdk2*, acting on downstream targets to allow transition from G_1 to S phase, subsequent cell division, and proliferation. Therefore, *Cdk2* is likely dispensable in the progression of PKD.

Another key observation from this study is that both *Cdk1* and *Cdk2* activity, and the activity of its partner cyclins, is downregulated in response to treatment with sirolimus. Previous studies, both preclinical and clinical, have demonstrated that, due to its inhibitory action on the mammalian target of rapamycin complex 1 (mTOR; a promoter of cell growth) [30], sirolimus treatment attenuates renal enlargement and cystic disease [20, 31–36]. This attenuating effect was consistent in the *jck* mouse model, and this reduced activity suggests that the therapeutic impact of sirolimus is, at least in part, mediated by Cdk

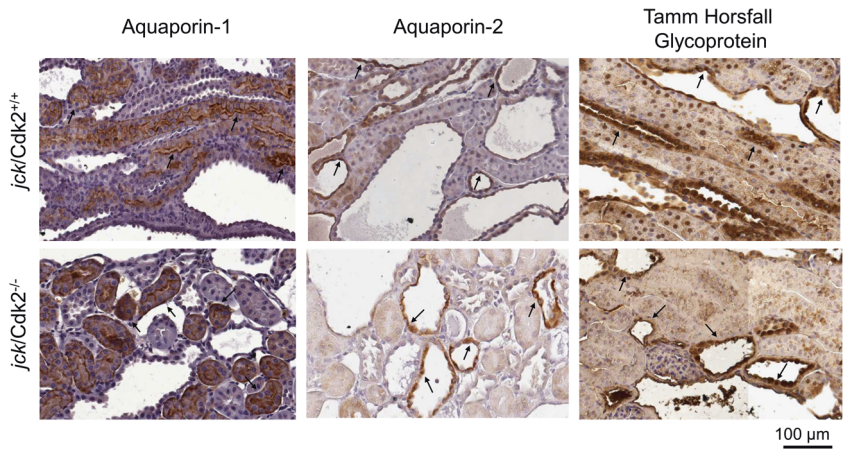

Fig. 11 Representative photomicrographs from juvenile cystic kidney (*jck*) disease mice in the absence or presence of cyclin-dependent kinase 2 (*Cdk2*) on day 84, showing the origin of the cystic epithelial cells. Magnification is ×20. Scale bar = 100 µm. Positive staining for aquaporin-1 indicates cyst origin from the proximal tubules and descending loop of Henle. Positive staining for aquaporin-2 indicates cyst origin from the collecting duct. Positive staining for Tamm Horsfall Glycoprotein indicates cyst origin from the ascending loop of Henle. *jck* juvenile cystic kidney, *Cdk* cyclin-dependent kinase.

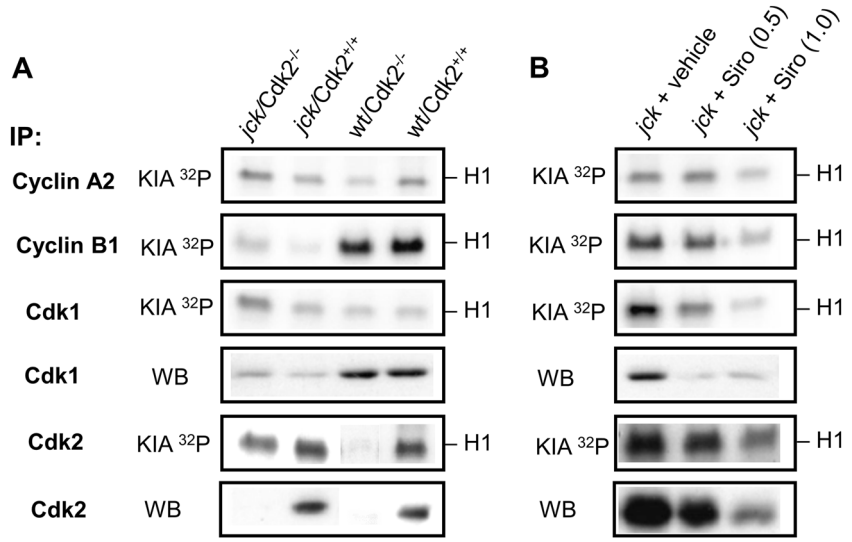

Fig. 12 The histone H1-kinase activity and western blot analysis of immunoprecipitated cyclins and cyclin-dependent kinases (Cdks) from juvenile cystic kidney (*jck*) disease mice in the absence or presence of cyclin-dependent kinase 2 (*Cdk2*), and with and without treatment with sirolimus. jck mice were treated in the absence or presence of cyclin-dependent kinase 2 (*Cdk2*) on day 84 **(a)**. *jck/Cdk2* mice received no treatment (vehicle) or treatment with sirolimus at 0.5 mg/kg body weight/day or 1.0 mg/kg body weight/day **(b)**. IP immunoprecipitation, KIA kinase assay, WB western blot, D day, wt wild-type, *jck* juvenile cystic kidney, *Cdk* cyclin-dependent kinase, Siro sirolimus, H1 histone H1.

inhibition. These results are consistent with Li et al. [37] who demonstrated that sirolimus treatment ameliorated cystic disease, by reducing the activity of cell-cycle-associated proteins, that is *Cdk1*, cyclin A, B, D1, and E, in a genetically orthologous murine model of human ADPKD (*Vil*-Cre; *Pkd2*$^{f3/f3}$). Though this finding emphasizes the functional significance of *Cdk1* in cystic disease, it also suggests a functional role for *Cdk2*, contrary to the results from our *Cdk2* knockout model.

This study also investigated *Cdk5* activity due to its hypothesized role in PKD progression. Previously, Husson et al. [10] demonstrated that *Cdk5* inhibition was effective in the treatment of renal cystic diseases, in part by reducing ciliary length and restoring tubular cell differentiation via its downstream effector, CRMP2. In vitro knockdown of *Cdk5* by small interfering RNA (siRNA) resulted in shortening of ciliary length in *jck* kidney epithelial cells, where increased ciliary length is known to contribute to pancreatic defects

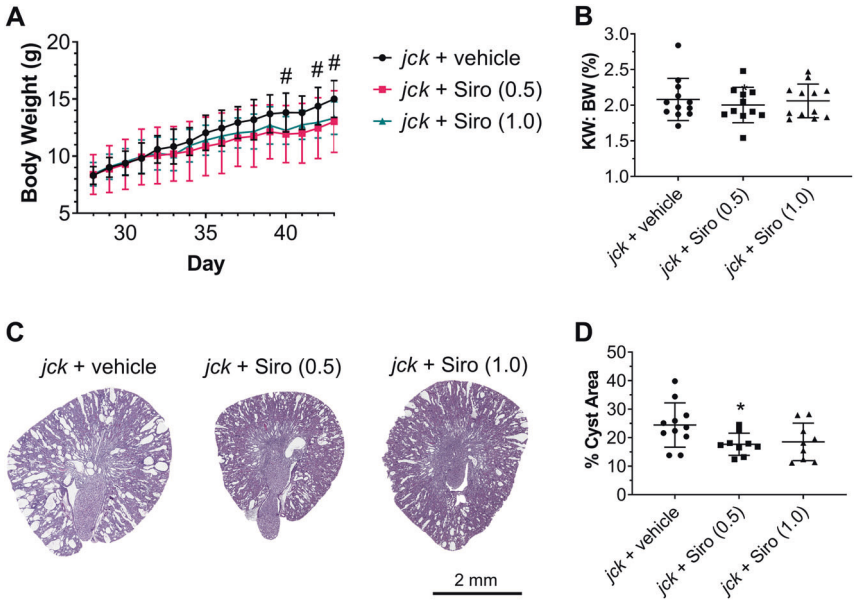

Fig. 13 Progression of cystic renal disease in male and female juvenile cystic kidney (*jck*) disease mice with and without treatment with sirolimus from day 28 until day 43. *jck*/Cdk2$^{+/+}$ mice received no treatment (vehicle) or treatment with sirolimus at 0.5 mg/kg body weight/day or 1.0 mg/kg body weight/day. a Body weight of male and female *jck* mice with and without sirolimus treatment from day 28 to day 43. **b** Two kidney weight to body weight (KW: BW) ratio of male and female *jck* mice with and without sirolimus treatment on day 43. **c** Representative whole-slide digital images of Periodic Acid Schiff (PAS)-stained sections of male and female *jck* mice with and without sirolimus treatment on day 43. **d** Percentage cyst area of male and female *jck* mice with and without sirolimus treatment on day 43. $^{\#}P < 0.05$ by one-way analysis of variance (ANOVA). $^{*}P < 0.05$ by 2-sample Mann–Whitney *U* test compared with age-matched *jck* mice with no treatment. *jck* juvenile cystic kidney, Siro sirolimus, KW: BW two kidney weight to body weight ratio.

associated with PKD [10, 38]. Furthermore, in vivo conditional knockout of *Cdk5* in *jck* mice from day 28 attenuated cystic disease (measured by KW: BW, cystic volume, and blood urea nitrogen), and resulted in the normalization of renal epithelial cell differentiation [10]. In this study, higher *Cdk5* expression was observed in *jck* mice compared with wild-type, consistent with Husson et al. [10]. However, in the *jck* mouse, *Cdk5* expression was attenuated by the absence of *Cdk2*. The reason for reduced *Cdk5* expression in the absence of *Cdk2* is not clear. In the present study, ciliary length was not measured, however, we found no changes in the expression of mesenchymal markers, vimentin and α-SMA, to suggest any therapeutic benefit in overall disease progression.

A key strength of this study is the generation of an in vivo Cdk2 knockout model of PKD, as previous studies have relied on pharmacological inhibition of Cdks. This model allowed the isolation of any changes in disease progression to *Cdk2* specifically, whereas pharmacological inhibitors tend to have a nonspecific mechanism of action. In particular, roscovitine acts on *Cdk1*, 2, 5, 7, and 9, and its activity persists in *Cdk2*-depleted cells, highlighting that the attenuation of cell proliferation and survival by the drug occurs through inhibition of multiple targets [39]. To date, this is the first study to examine a time course of Cdk and cyclin expression in a murine model of PKD, as well as determine the effect of an in vivo Cdk2 knockout on disease progression. The use of a kinase assay to examine the Cdk activity on a dynamic level, rather than a static measure of expression by western blot, further adds strength to our study findings.

The main limitation of this study was the lack of investigation into the in vivo effects of *Cdk2* ablation in late-stage PKD. Future investigations involving a conditional knock out of *Cdk2* in the *jck* mouse model or other models of PKD would provide further insight into the in vivo effects of *Cdk2* deficiency. It is possible that compensation by *Cdk1* only occurs when *Cdk2* is absent from birth. However, Husson et al. [10] found that the knockdown of *Cdk2* by siRNA had no effect on ciliary length in *jck* kidney epithelial cells, suggesting that *Cdk2* is still dispensable when inhibited later in life.

Future studies should be initially directed toward further examining the role of *Cdk2* and other Cdks involved in the cell cycle through conditional knockout studies, as ablation from birth is likely to activate compensation by *Cdk1*. It appears the most promising target is to examine the in vivo effects of *Cdk1* deficiency. However, *Cdk1* ablation from birth leads to embryonic lethality [27, 40], and conditional knock out has only been achieved in specific organs or

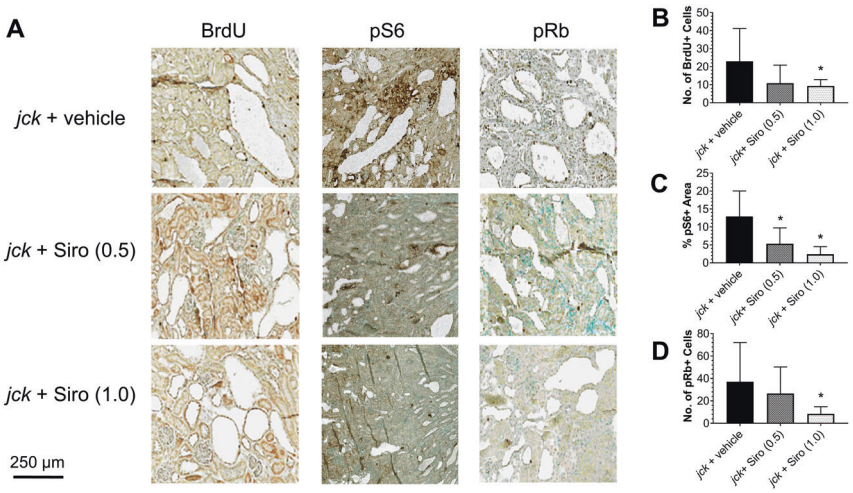

Fig. 14 Expression of bromodeoxyuridine (BrdU), phosphorylated S6 (pS6) ribosomal protein and phosphorylated retinoblastoma (pRb), measured by immunohistochemistry, in juvenile cystic kidney (*jck*) disease mice with and without treatment with sirolimus on day 43. a Representative photomicrographs of BrdU, pS6, and pRb positive staining. **b** Number of BrdU positive cyst-lining epithelial cells in five different 10x fields, as a measure of proliferation. **c** Percentage of pS6 positive staining area, as a measure of mTOR activation. **d** Number of pRb positive cyst-lining epithelial cells in five different 10x fields, as a measure of *Cdk2/4* activation. $^{*}P < 0.05$ by 2-sample Mann–Whitney *U* test compared with age-matched *jck* mice with no treatment. *jck* juvenile cystic kidney, Siro sirolimus.

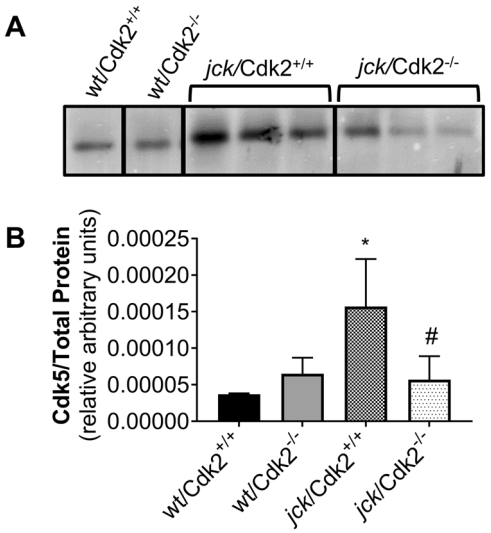

Fig. 15 Relative expression of cyclin-dependent kinase 5 (*Cdk5*), measured by western blot, using whole kidney tissue extracts from male and female wild-type (wt) and juvenile cystic kidney (*jck*) disease mice in the absence or presence of Cdk2 on day 84. a Representative blot of *Cdk5* expression. **b** Relative *Cdk5* expression. Band intensity was normalized to total protein intensity. $^{*}P < 0.05$ for comparisons to wild-type/*Cdk2*$^{+/+}$ animals, $^{\#}P < 0.05$ for comparisons between *jck*/*Cdk2*$^{+/+}$ and *jck*/Cdk2$^{-/-}$ mice by independent-samples *t*-test. wt wild-type, *jck* juvenile cystic kidney, *Cdk* cyclin-dependent kinase.

in vitro [40, 41], meaning it is likely not a feasible treatment option. Further investigation into other Cdks that are not typically associated with cell cycle, in particular, those inhibited by roscovitine, may also be of interest. *Cdk5* has demonstrated a potential role in PKD progression but was previously thought to only be involved in the development of neuronal function [6]. Bukanov et al. [13] also detected elevated levels of *Cdk7* and *Cdk9* in *jck* cystic kidneys compared with wild-type, warranting further investigation.

Finally, the feasibility and the efficacy of pharmacological Cdk inhibitors in the human ADPKD population needs further evaluation. For example, though sirolimus has demonstrated strong therapeutic potential in both preclinical and clinical studies, it has not been implemented in clinical practice due to limited adherence caused by side effects of mouth ulcers and hypercholesterolemia [36], and lack of efficacy at lower, more tolerable doses [32]. Furthermore, the evaluation of roscovitine treatment in patients with malignancies revealed significant side effects including nausea and vomiting, hypokalemia, elevations in serum creatinine and liver toxicity [42, 43], all of which would be particularly undesirable for a disease group with a predisposition to renal and hepatic impairment, that is, the PKD population. The identification of specific Cdk pharmacological targets, rather than administering nonspecific Cdk inhibitors, will be critical toward ameliorating these side effects and producing both feasible and effective treatment options. The evaluation of *Cdk4/6* inhibitors in the context of PKD may be useful, as roscovitine treatment reduced cyclin D2 and D3 expression (partners of *Cdk4/6*), normalized the phosphorylation of cyclin D, and resulted in dephosphorylation of pRb [13]. In particular, palbociclib (a selective *Cdk4/6* inhibitor) has been approved by the U.S. Food and Drug Administration for use in hormone receptor-positive advanced stage breast cancer based on phase III

clinical trials, which demonstrated improvement in survival outcomes with minimal side effects [44, 45].

This study investigated the role of *Cdk2* on the renal progression of PKD in *jck* mice. The results demonstrated that *Cdk2* ablation from birth did not reduce renal disease progression, most likely due to compensatory activity by *Cdk1*. No improvements in markers of disease progression, including cyst growth, inflammation, fibrosis, and renal impairment, were observed with *Cdk2* deficiency, and *Cdk2* activity was only maximal in the later stages of disease. These findings suggest that *Cdk2* is dispensable in PKD progression, and specifically targeting *Cdk2* is unlikely to improve disease outcomes. Future investigations should be aimed towards identifying effective and feasible drug targets by examining the specific in vivo roles of other Cdks and cyclins in the context of PKD.

Acknowledgements This study was supported by the National Health and Medical Research Council of Australia (Project Grant No 457575, 632647, 1164128, 1138533) and the PKD Foundation of Australia. JZ is supported by a Research Training Program Stipend from the University of Sydney. SS is supported by a grant from the PKD Foundation of Australia, and PK by the Biomedical Research Council of A*STAR (Agency for Science, Technology and Research), Singapore.

Compliance with ethical standards

Conflict of interest The authors declare that they have no conflict of interest.

References

1. Wilson PD. Mechanisms of disease: polycystic kidney disease. N Engl J Med. 2004;350:151–64.
2. Wilson PD. Therapeutic targets for polycystic kidney disease. Expert Opin Ther Targets. 2016;20:35–45.
3. Rangan GK, Tchan MC, Tong A, Wong AT, Nankivell BJ. Recent advances in autosomal-dominant polycystic kidney disease. Intern Med J. 2016;46:883–92.
4. Rangan GK, Lopez-Vargas P, Nankivell BJ, Tchan M, Tong A, Tunnicliffe DJ, et al. Autosomal dominant polycystic kidney disease: a path forward. Semin Nephrol. 2015;35:524–37.
5. Sanchez-Martinez C, Gelbert LM, Lallena MJ, de Dios A. Cyclin dependent kinase (CDK) inhibitors as anticancer drugs. Bioorg Med Chem Lett. 2015;25:3420–35.
6. Malumbres M, Barbacid M. Mammalian cyclin-dependent kinases. Trends Biochem Sci. 2005;30:630–41.
7. Berthet C, Kaldis P. Cell-specific responses to loss of cyclin-dependent kinases. Oncogene. 2007;26:4469–77.
8. Berthet C, Aleem E, Coppola V, Tessarollo L, Kaldis P. Cdk2 knockout mice are viable. Curr Biol. 2003;13:1775–85.
9. Ortega S, Prieto I, Odajima J, Martin A, Dubus P, Sotillo R, et al. Cyclin-dependent kinase 2 is essential for meiosis but not for mitotic cell division in mice. Nat Genet. 2003;35:25–31.
10. Husson H, Moreno S, Smith LA, Smith MM, Russo RJ, Pitstick R, et al. Reduction of ciliary length through pharmacologic or genetic inhibition of CDK5 attenuates polycystic kidney disease in a model of nephronophthisis. Hum Mol Genet. 2016;25:2245–55.
11. Bhunia AK, Piontek K, Boletta A, Liu L, Qian F, Xu PN, et al. PKD1 induces p21(waf1) and regulation of the cell cycle via direct activation of the JAK-STAT signaling pathway in a process requiring PKD2. Cell. 2002;109:157–68.
12. Felekkis KN, Koupepidou P, Kastanos E, Witzgall R, Bai CX, Li L, et al. Mutant polycystin-2 induces proliferation in primary rat tubular epithelial cells in a STAT-1/p21-independent fashion accompanied instead by alterations in expression of p57KIP2 and Cdk2. BMC Nephrol. 2008;9:10.
13. Bukanov NO, Smith LA, Klinger KW, Ledbetter SR, Ibraghimov-Beskrovnaya O. Long-lasting arrest of murine polycystic kidney disease with CDK inhibitor roscovitine. Nature. 2006;444:949–52.
14. Bukanov NO, Moreno SE, Natoli TA, Rogers KA, Smith LA, Ledbetter SR, et al. CDK inhibitors R-roscovitine and S-CR8 effectively block renal and hepatic cystogenesis in an orthologous model of ADPKD. Cell Cycle. 2012;11:4040–6.
15. Liu S, Lu W, Obara T, Kuida S, Lehoczky J, Dewar K, et al. A defect in a novel Nek-family kinase causes cystic kidney disease in the mouse and in zebrafish. Development. 2002;129:5839–46.
16. Sohara E, Luo Y, Zhang J, Manning DK, Beier DR, Zhou J. Nek8 regulates the expression and localization of polycystin-1 and polycystin-2. J Am Soc Nephrol. 2008;19:469–76.
17. McCooke JK, Appels R, Barrero RA, Ding A, Ozimek-Kulik JE, Bellgard MI, et al. A novel mutation causing nephronophthisis in the Lewis polycystic kidney rat localises to a conserved RCC1 domain in Nek8. BMC Genom. 2012;13:393-.
18. Atala A, Freeman MR, Mandell J, Beier DR. Juvenile cystic kidneys (jck): A new mouse mutation which causes polycystic kidneys. Kidney Int. 1993;43:1081–5.
19. Smith LA, Bukanov NO, Husson H, Russo RJ, Barry TC, Taylor AL, et al. Development of polycystic kidney disease in juvenile cystic kidney mice: Insights into pathogenesis, ciliary abnormalities, and common features with human disease. J Am Soc Nephrol. 2006;17:2821–31.
20. Shillingford JM, Piontek KB, Germino GG, Weimbs T. Rapamycin ameliorates PKD resulting from conditional inactivation of Pkd1. J Am Soc Nephrol. 2010;21:489–97.
21. Schonthal AH. Measuring cyclin-dependent kinase activity. Methods Mol Biol. 2004;281:105–24.
22. Satyanarayana A, Hilton MB, Kaldis P. p21 Inhibits Cdk1 in the absence of Cdk2 to maintain the G1/S phase DNA damage checkpoint. Mol Biol Cell. 2008;19:65–77.
23. Choi HJ, Lin JR, Vannier JB, Slaats GG, Kile AC, Paulsen RD, et al. NEK8 links the ATR-regulated replication stress response and S phase CDK activity to renal ciliopathies. Mol Cell. 2013;51:423–39.
24. Ta MHT, Schwensen KG, Liuwantara D, Huso DL, Watnick T, Rangan GK. Constitutive renal Rel/nuclear factor-κB expression in Lewis polycystic kidney disease rats. World J Nephrol. 2016;5:339–57.
25. Cassini MF, Kakade VR, Kurtz E, Sulkowski P, Glazer P, Torres R, et al. Mcp1 Promotes Macrophage-Dependent Cyst Expansion in Autosomal Dominant Polycystic Kidney Disease. J Am Soc Nephrol. 2018;29:2471–81.
26. Aleem E, Kaldis P, Kiyokawa H. Cdc2-cyclin E complexes regulate the G1/S phase transition. Nat Cell Biol. 2005;7:831–6.
27. Santamaria D, Barriere C, Cerqueira A, Hunt S, Tardy C, Newton K, et al. Cdk1 is sufficient to drive the mammalian cell cycle. Nature. 2007;448:811–5.
28. Padmakumar VC, Aleem E, Berthet C, Hilton MB, Kaldis P. Cdk2 and Cdk4 activities are dispensable for tumorigenesis caused by the loss of p53. Mol Cell Biol. 2009;29:2582–93.
29. Bienvenu F, Jirawatnotai S, Elias JE, Meyer CA, Mizeracka K, Marson A, et al. Transcriptional role of cyclin D1 in development revealed by a genetic-proteomic screen. Nature. 2010;463:374–8.

30. Ibraghimov-Beskrovnaya O, Natoli TA. mTOR signaling in polycystic kidney disease. Trends Mol Med. 2011;17: 625–33.
31. Tao Y, Kim J, Schrier RW, Edelstein CL. Rapamycin markedly slows disease progression in a rat model of polycystic kidney disease. J Am Soc Nephrol. 2005;16:46–51.
32. Serra AL, Poster D, Kistler AD, Krauer F, Raina S, Young J, et al. Sirolimus and kidney growth in autosomal dominant polycystic kidney disease. N Engl J Med. 2010;363:820–9.
33. Wu M, Wahl PR, Le Hir M, Wäckerle-Men Y, Wüthrich RP, Serra AL. Everolimus retards cyst growth and preserves kidney function in a rodent model for polycystic kidney disease. Kidney Blood Press Res. 2007;30:253–9.
34. Gattone VH, Sinders RM, Hornberger TA, Robling AG. Late progression of renal pathology and cyst enlargement is reduced by rapamycin in a mouse model of nephronophthisis. Kidney Int. 2009;76:178–82.
35. Walz G, Budde K, Mannaa M, Nürnberger J, Wanner C, Sommerer C, et al. Everolimus in patients with autosomal dominant polycystic kidney disease. N Engl J Med. 2010;363:830–40.
36. Perico N, Antiga L, Caroli A, Ruggenenti P, Fasolini G, Cafaro M, et al. Sirolimus therapy to halt the progression of ADPKD. J Am Soc Nephrol. 2010;21:1031–40.
37. Li A, Fan S, Xu Y, Meng J, Shen X, Mao J, et al. Rapamycin treatment dose-dependently improves the cystic kidney in a new ADPKD mouse model via the mTORC1 and cell-cycle-associated CDK1/cyclin axis. J Cell Mol Med. 2017;21: 1619–35.
38. Cano DA, Murcia NS, Pazour GJ, Hebrok M. orpk mouse model of polycystic kidney disease reveals essential role of primary cilia in pancreatic tissue organization. Development. 2004;131: 3457–67.
39. Sp Bach, Knockaert M, Reinhardt J, Lozach O, Schmitt S, Baratte B, et al. Roscovitine targets, protein kinases and pyridoxal kinase. J Biol Chem. 2005;280:31208–19.
40. Diril MK, Ratnacaram CK, Padmakumar VC, Du T, Wasser M, Coppola V, et al. Cyclin-dependent kinase 1 (Cdk1) is essential for cell division and suppression of DNA re-replication but not for liver regeneration. Proc Natl Acad Sci USA. 2012;109:3826–31.
41. Adhikari D, Zheng W, Shen Y, Gorre N, Ning Y, Halet G, et al. Cdk1, but not Cdk2, is the sole Cdk that is essential and sufficient to drive resumption of meiosis in mouse oocytes. Hum Mol Genet. 2012;21:2476–84.
42. Benson C, White J, De Bono J, O'Donnell A, Raynaud F, Cruickshank C, et al. A phase I trial of the selective oral cyclin-dependent kinase inhibitor seliciclib (CYC202; -Roscovitine), administered twice daily for 7 days every 21 days. Br J Cancer. 2007;96:29–37.
43. Le Tourneau C, Faivre S, Laurence V, Delbaldo C, Vera K, Girre V, et al. Phase I evaluation of seliciclib (R -roscovitine), a novel oral cyclin-dependent kinase inhibitor, in patients with advanced malignancies. Eur J Cancer. 2010;46:3243–50.
44. Cristofanilli M, Turner NC, Bondarenko I, Ro J, Im SA, Masuda N, et al. Fulvestrant plus palbociclib versus fulvestrant plus placebo for treatment of hormone-receptor-positive, HER2-negative metastatic breast cancer that progressed on previous endocrine therapy (PALOMA-3): final analysis of the multicentre, double-blind, phase 3 randomised controlled trial. Lancet Oncol. 2016;17:425–39.
45. Finn RS, Crown JP, Lang I, Boer K, Bondarenko IM, Kulyk SO, et al. The cyclin-dependent kinase 4/6 inhibitor palbociclib in combination with letrozole versus letrozole alone as first-line treatment of oestrogen receptor-positive, HER2-negative, advanced breast cancer (PALOMA-1/TRIO-18): a randomised phase 2 study. Lancet Oncol. 2015;16:25–35.